Generalized Theoretical and Practical Treatment of the Kinetics of an Enzyme-Catalyzed Reaction in the Presence of an Enzyme Equimolar Irreversible Inhibitor†

Marko Goličnik* and Jure Stojan

Institute of Biochemistry, Medical Faculty, University of Ljubljana, Vrazov trg 2, 1000 Ljubljana, Slovenia

Received March 19, 2003

We revisit a previous analysis of the classical Michaelis−Menten enzyme reaction for the case in which the free enzyme incurs the loss of its activity by an irreversible inhibitor concentration dependent but time unaltered rate constant (see Goličnik, M. *J. Chem. Inf. Comput. Sci.* **2002**, *42*, 157−161). We study the kinetic model of an enzyme-catalyzed reaction in the presence of an equimolar irreversible inhibitor showing a time dependent inactivation rate constant because of considerable inhibitor amount depletion during the course of the reaction. We show that an analytical solution containing the nonelementary Gauss hypergeometric function can be found for the reactants in equation Φ of an implicit type that precludes direct calculation of the extent of reaction at any time. The transformation theory of the hypergeometric function is used to obtain rapidly convergent power series, and for the root calculation of equation Φ the divergence-proof root bracketing algorithm according to Van Wijngaarden-Dekker-Brent is performed. Numerically generated data are analyzed according to this mathematical procedures, and the results are compared with ones obtained by the numerical integration treatment.

1. INTRODUCTION

The Michaelis−Menten framework[1] has proven to be a simple yet powerful approach to describe many basic enzyme processes,[2,3] resulting in the hyperbolic equation which transforms to a double-reciprocal linear plot[4] for simple estimation of the kinetic parameters. Despite this easy to be solved mathematical procedure the kinetic analysis with the use of complete time courses rather than initial rates has several often quoted advantages: (i) inherently more information is available in each experiment;[5,6] (ii) the need to perform more or less subjective calculations of initial rates is eliminated;[6,7] (iii) the data used, primarily in the central portion of the progress curves, should be more reliable;[6−8] products need not be added in order to obtain product inhibition effects etc. There have been many proposed numerical algorithms for integrated rate equation root solving and consequently for fitting the equation to the experimental data.[5,6,9,10] It has been shown recently by Goudar et al.[10] that newly developed numerical techniques for direct solution finding of the integrated Michaelis−Menten equation are proven to be more efficient than numerical integration of appropriate differential equations that might be computationally intensive and therefore relatively slow.

Progress curve analysis, despite the difficulties encountered, seems especially convenient when studying slow enzyme inhibition processes in the presence of a slow acting reversible inhibitor[11,12] as well as by a tight binding ligand[13,14] or an irreversible inhibitor. Recently, we explored the reaction of acetylcholinesterase with 7-(methylethoxyphosphinyloxy)-1-methyl-quinolinium iodide (MEPQ), the potent irreversible organophosphate agent for serine enzymes, in the presence of the substrate acetylthiocholine by following the time course of the reaction product thiocholine.[15] It has been demonstrated that the progress curves obtained in latter work at inhibitor concentrations at least 10 times higher than those of an enzyme could be described by the exponential integral nonelementary function in an equation of an implicit type that precludes direct computation of the extent of the reaction at any time. Therefore an appropriate numerical root finding method has been proposed and efficiently applied.

In the present paper we reexamine the reaction between a Michaelis−Menten enzyme and a very potent irreversible inhibitor of free enzyme in detail, resulting in a mathematical formalism that is valid without inhibitor concentration exception. This means that it applies at any inhibitor concentration even when the enzyme is its reaction partner in a near stoichiometric amount. For such a kinetic model the derivation of an integrated rate equation, needed for the analytical description of progress curves, is possible by solving the system of appropriate differential equations. The exact solution which includes the Gauss hypergeometric nonelementary function is an implicit equation, so that the practical computations had to be relied on approximate numerical methods.

2. THEORY

1. Basic Enzyme Kinetics. We consider a biochemical reaction in which an enzyme ([*E*]) reacts reversibly with a substrate ([*S*]) to form an intermediate noncovalent enzyme−substrate complex ([*ES*]). The complex [*ES*] then irreversibly breaks down into the original enzyme and an altered substrate

† Abbreviations used: WDB's algorithm, Van Wijngaarden-Dekker-Brent's algorithm.

* Corresponding author phone: +386-(0)-1-5437651; fax: +386-(0)-1-5437641; e-mail: marko.golicnik@mf.uni-lj.si.

10.1021/ci0304021 CCC: $25.00
Published on Web 08/13/2003

molecule called the product ([*P*]) that shows no inhibition effects on the enzyme.

Scheme 1

$$E + S \underset{k_{-1}}{\overset{k_{+1}}{\rightleftharpoons}} ES \xrightarrow{k_{+2}} E + P$$

k_{+1} is a bimolecular rate constant, but k_{-1} and k_{+2} are monomolecular rate constants. In the framework based on the standard quasi-steady-state assumption[16] the Michaelis−Menten equation can be derived

$$v_0 = \frac{V_{max}[S]}{K_M + [S]} \tag{1}$$

and this hyperbolic function of the initial reaction velocity (v_0) with substrate concentration ([*S*]) allows one to estimate the reaction parameters, namely the Michaelis constant $K_M = (k_{-1} + k_{+2})/k_{+1}$ and the maximum velocity $V_{max} = k_{+2}[E]_0$.

An attractive alternative to the initial rate methods for the determination of kinetic parameters is the analysis of the entire time courses of enzyme-catalyzed reactions.[5−7,9,10] The progress curves are described by the so-called integrated Michaelis−Menten equation

$$[S]_0 - [S]_t - K_M ln\left(\frac{[S]_t}{[S]_0}\right) = V_{max} t \tag{2}$$

where $[S]_t$ represents the concentration of substrate at any time t and $[S]_0$ is total initial substrate concentration. It is obvious from eq 2 that $[S]_t$ cannot be explicitely (directly) calculated, and therefore several numerical methods were proposed for finding the root ($[S]_t$) of eq 2.[6,15]

When an irreversible inhibitor ([*I*]) competes with the substrate for the active site of a free enzyme, the consequence is an uneffective covalently modified enzyme ([*E*′]). The chemical events going on in such a system can be represented by Scheme 2

Scheme 2

$$E' \xleftarrow{j} I + E + S \underset{k_{-1}}{\overset{k_{+1}}{\rightleftharpoons}} ES \xrightarrow{k_{+2}} E + P$$

where j is bimolecular rate constant. It has been reported recently[15] that the product concentration $[P]_t$ at any time could be evaluated by the exponential integral nonelementary implicit function under the condition that the free enzyme concentration decreases according to a time unaltered rate constant. This condition is attained when the inhibitor concentration does not change essentially during the course of reaction. It means that the inhibitor depletion is negligible at any time ($[I]_t$) and is practically equal to the initial total inhibitor concentration ($[I]_0$ in the text), and therefore the ratio $[I]_0/[E]_0$ throughout the reaction is high.

If this basic assumption is violated, as in the case of very potent inhibitors, a different mathematical treatment must be applied. Two coupled differential equations define the rates of enzyme inactivation and substrate utilization according to Scheme 2

$$\frac{d[E']}{dt} = \frac{j([E]_0 - [E'])\,([I]_0 - [E'])}{\left(1 + \frac{[S]}{K_M}\right)} \tag{3}$$

$$\frac{d[S]}{dt} = -\frac{k_{+2}([E]_0 - [E'])\,[S]}{K_M\left(1 + \frac{[S]}{K_M}\right)} \tag{4}$$

It should be reminded that the eqs 3 and 4 are valid only when [*ES*] is treated under steady-state assumption (see refs 2, 9, 15).

2. Model System in Nondimensional Form. It is always advantageous to express the model system in nondimensional terms. By converting to nondimensional variables and parameters, we can then consider quantities on an absolute scale, independent of specific units. Such a procedure gives immediately a measure of relative magnitudes of various contributions to the rate equations.

The variables were set as follows: $s = [S]/[S]_0$, $T = k_{+2}t$, and $e' = [E']/[E]_0$ where s, T, and e' are now dimensionless. Equations 3 and 4 can be transformed to the following two dimensionless differential equations

$$\frac{de'}{dT} = \frac{j[I]_0\,(1 - e')\,(1 - \mu e')}{k_{+2}\,(1 + \lambda s)} \tag{5}$$

$$\frac{ds}{dT} = -\frac{\kappa\,(1 - e')s}{(1 + \lambda s)} \tag{6}$$

where $\kappa = [E]_0/K_M$, $\lambda = [S]_0/K_M$, and $\mu = [E]_0/[I]_0$. While these equations cannot be integrated with respect to dimensionless time T, the division of eq 5 by eq 6 gives

$$\frac{de'}{ds} = -\frac{j[I]_0\,(1 - \mu e')}{k_{+2}\kappa s} \tag{7}$$

Equation 7 gives upon integration an expression relating e' and s

$$e' = \frac{(1 - s^{\omega})}{\mu} \tag{8}$$

where ω is jK_M/k_{+2}. It should be emphasized that the relation $\mu \lessgtr 1$ determinates two types of progress curves

Case A

$$\mu \geq 1 \Rightarrow s_\infty = 0 \tag{9}$$

Case B

$$\mu < 1 \Rightarrow s_\infty = (1 - \mu)^{1/\omega} \tag{10}$$

By putting the right side of eq 8 in eq 6 the following rate equation is obtained

$$\frac{ds}{dT} = -\frac{\kappa s\,(\mu - 1 + s^{\omega})}{\mu\,(1 + \lambda s)} \tag{11}$$

Upon integration, an analytical solution is an implicit nonelementary function

$$\Phi_1 = \Phi_1^{\alpha} + \Phi_1^{\beta} + \Phi_1^{\gamma} = 0 \tag{12}$$

where

$$\Phi_1^{\alpha} = \frac{1}{\omega} ln\left(\frac{\mu s^{\omega}}{(\mu - 1 + s^{\omega})}\right) \tag{13}$$

$$\Phi_1^{\beta} = \lambda\left(s \cdot {}_2F_1\left[1, \frac{1}{\omega}; 1 + \frac{1}{\omega}; -\frac{s^{\omega}}{\mu - 1}\right] - {}_2F_1\left[1, \frac{1}{\omega}; 1 + \frac{1}{\omega}; -\frac{1}{\mu - 1}\right]\right) \tag{14}$$

$$\Phi_1^{\gamma} = \frac{\kappa(\mu - 1)}{\mu} T \tag{15}$$

${}_2F_1[a, b; c; z]$ is Gauss hypergeometric function.

Equation 12 is a general solution of differential eq 11, but we should emphasize a special case in which eq 12 does not apply. When $\mu = 1$ ($[I]_0 = [E]_0$), the integration of eq 11 leads to the following equation

$$\Phi_1' = \frac{1}{\omega}(1 - s^{-\omega}) + \frac{\lambda}{(\omega - 1)}(1 - s^{1-\omega}) + \kappa T = 0 \tag{16}$$

Another special case arises when the inhibitor in the reaction mixture is either inactive ($j = 0$) or absent ($[I]_0 = 0$). Therefore Scheme 2 reduces to Scheme 1, and consequently the progress curves are described by eq 2 which is in its nondimensionalised form as follows

$$\Phi_1'' = \lambda(1 - s) - ln s - \kappa T = 0 \tag{17}$$

3. Gauss Hypergeometric Function. The hypergeometric function ${}_2F_1[a, b; c; z]$ is defined as an analytic continuation of the so-called hypergeometric series

$${}_2F_1[a, b; c; z] = \sum_{n=0}^{\infty} \frac{(a)_n (b)_n}{(c)_n n!} z^n \tag{18}$$

where $(a)_n$, $(b)_n$, and $(c)_n$ are Pochhammer's symbols (see Appendix). The circle of its convergence is the unit circle $|z| \leq 1$, but one's interest in the function is often not confined to this region, as also in our work. For z outside the circle of convergence, it is necessary to transform z in such a way that the hypergeometric function can be expressed in terms of other hypergeometric functions of a new argument w so that $|w| < 1$. To do this, the real axis was divided into six intervals as shown in Table 1.[18,19] In each case, a new independent variable w lies in the range between zero and one-half, so that the series in powers of w not only converge but also converge rapidly. Although the evaluation of ${}_2F_1[a, b; c; z]$ function by this method has proven efficient, many other algorithms such as path integration,[20] binary splitting method,[21] or FEE (Fast E-function Evaluation) method[22−24] have also been proposed.

The argument z of hypergeometric function appearing in eq 12 is either $-s^{\omega}/(\mu - 1)$ or $-1/(\mu - 1)$ and consequently the value of this argument depends on the magnitude of μ. If $\mu > 1$, then

$$-1/(\mu - 1) \leq -s^{\omega}/(\mu - 1) \leq 0 \tag{19}$$

otherwise, when $\mu < 1$, then

$$-1/(\mu - 1) \geq -s^{\omega}/(\mu - 1) \geq 1 \tag{20}$$

It follows, that our interest is only focused on cases *I*, *II*, *V*, and *VI* in Table 1. Each term in these formulas (except in case *II*) has a pole either when $a - b = \pm n$ or when $c - a - b = \pm n$. n means an integer. One of the terms in transformed equations diverges due to a gamma function of negative argument in the numerator, and the other diverges because the third parameter in ${}_2F_1$ is a negative integer. According to a finite difference technique[25] these divergences can be removed approximately.

In eq 12 we assumed $a - b = 1 - 1/\omega$. In reality, it is unexpected that this expression would be a whole number. Therefore we additionally omitted pole problems in cases *I* and *VI*. The problem arises with transformated formula in case *V* because $c - a - b$ is equal to zero for ${}_2F_1$ functions in eq 12. We solved this case by two additional generally valid formulas[19,26] (i) for $z \leq 1.5$

$${}_2F_1[a, b; a + b; z] = \mathscr{R}\left(\frac{\Gamma(a + b)}{\Gamma(a)\Gamma(b)} \cdot \sigma\right) \tag{21}$$

$$\sigma = \sum_{n=0}^{\infty} \frac{(a)_n (b)_n}{(n!)^2} [2\Psi(n + 1) - \Psi(a + n) - \Psi(b + n) - ln(1 - z)](1 - z)^n \tag{22}$$

where Ψ is digamma function (see Appendix) and (ii) for $z > 1.5$

$${}_2F_1[a, b; b + 1; z] = b z^{-b} B_z(b, 1 - a) \tag{23}$$

where B_z is incomplete beta function (see Appendix). Both linear transformations are suitable and useful for computing hypergeometric functions in eq 12. All finally derived and applied transformated equations at appropriate intervals are shown in Table 2. The criterion for the number of sufficient terms in partial sum to attain sufficient accuracy are also given in Table 2.

3. METHODS

1. Data Simulation. The progress curves at various substrate concentrations (λ) and different enzyme−inhibitor concentration ratios (μ) were numerically simulated by using eqs 12, 16, and 17 accordingly. Each individual data point at any time t was computed by FindRoot numerical procedure using *Mathematica* software package.[27] To approach the simulation to more realistic circumstances we added a simulated error with mean zero and a specified standard deviation to each simulated data point (see Figure 1) using a random normal distribution.

2. Data Analysis. Implicit eqs 12, 16, and 17 preclude direct calculation of substrate remaining or product formed at any time. So, the dependent variable s has to be numerically approximated. The Newton−Raphson method is very efficient for the case of eq 17 when this equation is rearranged to a more appropriate form defined along the entire nondimensionalized substrate concentration interval [0,1][6,7,15]

$$\Phi_2'' = s - e^{(\lambda(1-s) - \kappa T)} \tag{24}$$

Table 1. Transformations of Hypergeometric Function[a,b]

Case	Interval	Transformation	Identity ${}_2F_1(a,b;c;z) =$	Divergence
I	$-\infty< z <-1$	$w=\frac{1}{1-z}$	$w^a\frac{\Gamma(c)\Gamma(b-a)}{\Gamma(b)\Gamma(c-a)}{}_2F_1(a,c-b;a-b+1;w)+w^b\frac{\Gamma(c)\Gamma(a-b)}{\Gamma(a)\Gamma(c-b)}{}_2F_1(b,c-a;b-a+1;w)$	$a-b=n^{**}$
II	$-1\le z <0$	$w=\frac{z}{z-1}$	$(1-w)^a{}_2F_1(a,c-b;c;w)$	-
III	$0\le z \le 0.5$	$w=z$	${}_2F_1(a,b;c;z)$	-
IV	$0.5 < z \le 1$	$w=1-z$	$\frac{\Gamma(c)\Gamma(c-a-b)}{\Gamma(c-a)\Gamma(c-b)}{}_2F_1(a,b;a+b-c+1;w)+w^{(c-a-b)}\frac{\Gamma(c)\Gamma(a+b-c)}{\Gamma(a)\Gamma(b)}{}_2F_1(c-a,c-b;c-a-b+1;w)$	$c-a-b=n^{**}$
*V**	$1 < z \le 2$	$w=1-\frac{1}{z}$	$(1-w)^a\frac{\Gamma(c)\Gamma(c-a-b)}{\Gamma(c-a)\Gamma(c-b)}{}_2F_1(a,a-c+1;a+b-c+1;w)+(1-w)^b\lvert w\rvert^{(c-a-b)}e^{-i\pi(c-a-b)}\frac{\Gamma(c)\Gamma(a+b-c)}{\Gamma(a)\Gamma(b)}{}_2F_1(1-b,c-b;c-a-b+1;w)$	$c-a-b=n^{**}$
*VI**	$2 < z < +\infty$	$w=\frac{1}{z}$	$\lvert w\rvert^a e^{i\pi a}\frac{\Gamma(c)\Gamma(b-a)}{\Gamma(b)\Gamma(c-a)}{}_2F_1(a,a-c+1;a-b+1;w)+\lvert w\rvert^b e^{i\pi b}\frac{\Gamma(c)\Gamma(a-b)}{\Gamma(a)\Gamma(c-b)}{}_2F_1(b-c+1,b;b-a+1;w)$	$a-b=n^{**}$

[a] An asterisk (*) denotes the following: in case V and VI the identity are in fact equal to $\lim_{\epsilon\to 0^+}{}_2F_1(a,\ b;\ c;\ z+i\epsilon)$. [b] Two asterisks (**) denote the following: *n* means an integer number.

Table 2. Transformations of Hypergeometric Function in Eq 12[a,b]

Interval	Transformation	Identity ${}_2F_1(1,\frac{1}{\omega},1+\frac{1}{\omega};z) =$	Convergence*
$-\infty< z <-1$	$w=\frac{1}{1-z}$	$\frac{\pi}{\omega sin\left(\frac{\pi}{\omega}\right)}w^{\frac{1}{\omega}}(1-w)^{-\frac{1}{\omega}}+\frac{sin\left(\frac{\pi}{\omega}\right)}{(\omega-1)sin\left(\pi\left(\frac{1}{\omega}-1\right)\right)}w\sum_{n=0}^{\infty}\frac{n!}{\left(2-\frac{1}{\omega}\right)_n}w^n$	$\frac{N!\left(N+2-\frac{1}{\omega}\right)}{\left(2-\frac{1}{\omega}\right)_N\left(N+2-\frac{1}{\omega}-(N+1)w\right)}w^N<\epsilon^{**}$
$-1\le z <0$	$w=\frac{z}{z-1}$	$(1-w)\sum_{n=0}^{\infty}\frac{n!}{\left(1+\frac{1}{\omega}\right)_n}w^n$	$\frac{N!}{\left(1+\frac{1}{\omega}\right)_N(1-w)}w^N<\epsilon$
$1 < z \le 1.5$	$w=z-1$	$\frac{1}{\omega}\sum_{n=0}^{\infty}(-1)^n\frac{\left(\frac{1}{\omega}\right)_n}{n!}\left[\Psi(n+1)-\Psi\left(n+\frac{1}{\omega}\right)-lnw\right]w^n$	$\frac{\left(\frac{1}{\omega}\right)_N}{N!}\left[\Psi(N+1)-\Psi\left(N+\frac{1}{\omega}\right)-lnw\right]w^N<\epsilon$
$1.5 < z$	$w=\frac{1}{z}$	$\frac{1}{\omega}w^{\frac{1}{\omega}}\left(\frac{\pi cos\left(-\frac{\pi}{\omega}\right)}{sin\left(\frac{\pi}{\omega}\right)}+w^{1-\frac{1}{\omega}}\sum_{n=0}^{\infty}\frac{\left(1-\frac{1}{\omega}\right)_n}{\left(2-\frac{1}{\omega}\right)_n}w^n\right)$	$\frac{\left(1-\frac{1}{\omega}\right)}{\left(N+1-\frac{1}{\omega}\right)(1-w)}w^N<\epsilon$

[a] An asterisk (*) denotes the following: the remainder of individual series R_N is smaller than ϵ (Cauchy convergence principle) when the following relations are satisfied. [b] Two asterisks (**) denote the following: additional condition is $1/\omega < (n+1)(1-w)+1$.

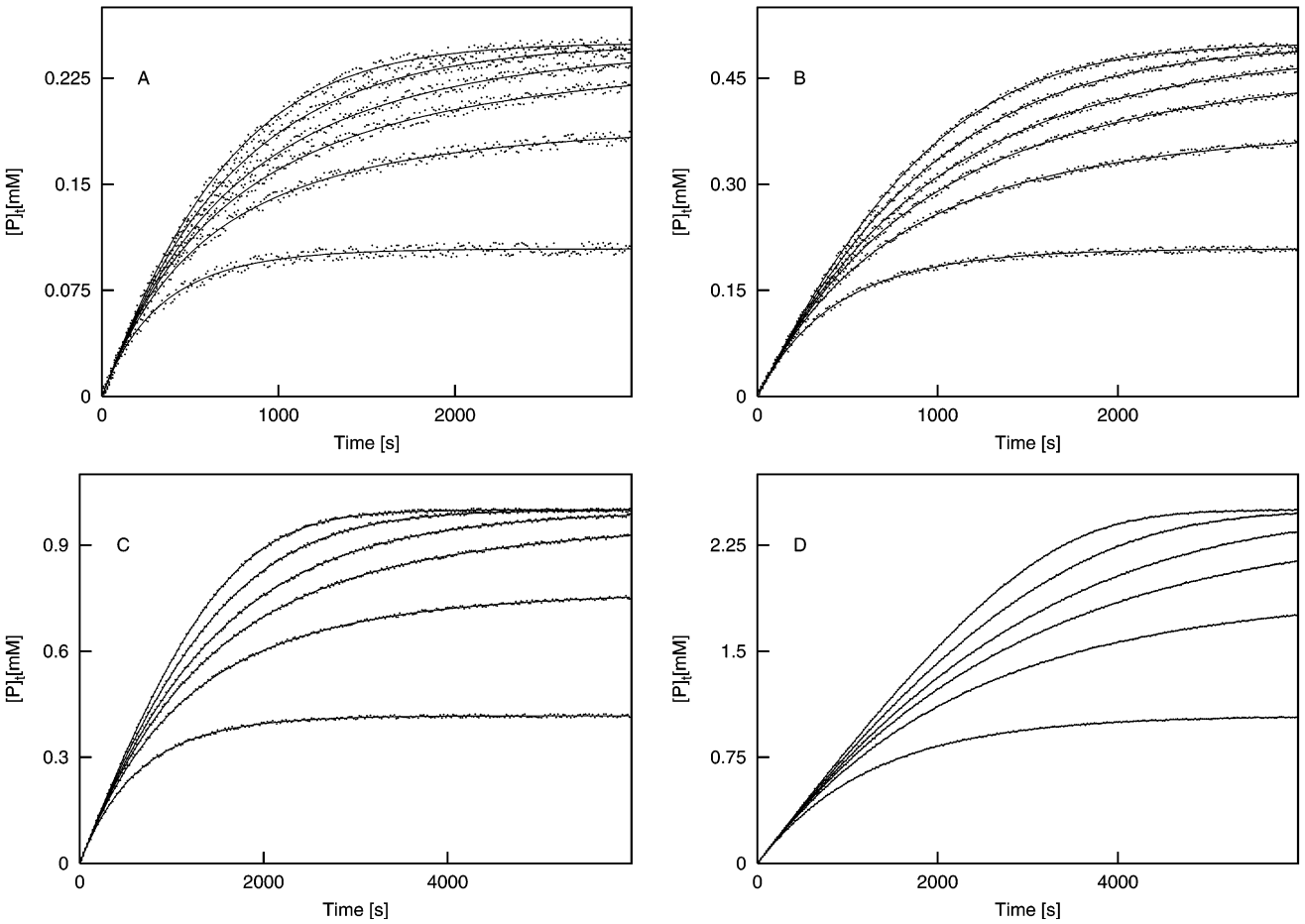

Figure 1. Simulated progress curves at different total substrate concentrations $[S]_0$ − (A) 0.25 mM, (B) 0.5 mM, (C) 1 mM, (D) 2.5 mM and by the following kinetic parameters − $k_{+2} = 1000\ s^{-1}$, $K_M = 0.5$ mM and $j = 10^6\ M^{-1}\ s^{-1}$. Total enzyme concentration is 1*nM* in all cases. In all four labeled figures the inhibitor concentration increases in turn 0 nM, 0.35 nM, 0.7 nM, 1 nM, 1.5 nM, and 3 nM referring to individual progress curves from up to down.

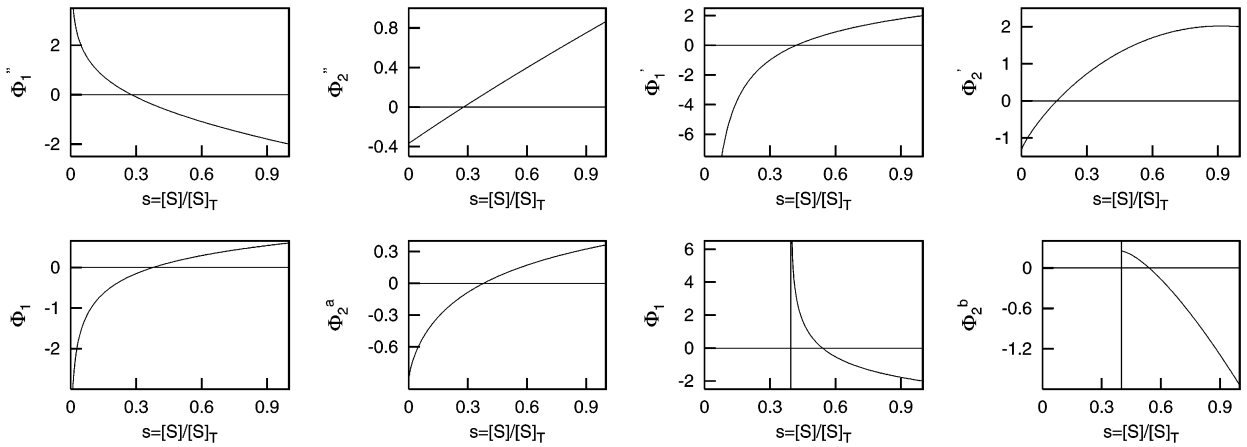

Figure 2. Dependence of Φ_1, Φ_2^a, Φ_2^b, Φ_1', Φ_1'', Φ_2', and Φ_2'' upon $s = [S]/[S]_0$. The kinetic parameters are the same as in Figure 1. $[S]_0 =$ 0.5 mM and $t = 1000$ s in all cases. For Φ_1''/Φ_2'' pair the inhibitor concentration is 0 nM ($\mu = \infty$), for Φ_1'/Φ_2' 1 nM (equal to $[E]_0$, $\mu = 1$), for Φ_1/Φ_2^a 0.7 nM ($\mu = 10/7$) and for Φ_1/Φ_2^b 1.5 nM ($\mu = 2/3$).

This equation using the Newton−Raphson algorithm was applied for root finding in case of progress curves obtained in the absence of the inhibitor.

The rearrangements of formulas 13 and 14 were also necessary, but the final form of these two equations depended on the size of $\mu \left(\lessgtr 1\right)$ or consequently within range where the root of s occurred. It should be emphasized that when $\mu > 1$ the root of s at any time t is to be found between zero and one ([0,1] interval, see eq 9) and eq 12 is valid on the entire interval. But for the efficient numerical approximation of s the following rearrangement had to be done (see also Figure 2)

$$\Phi_2^a = \frac{\mu s^\omega}{(\mu - 1 + s^\omega)} - e^{-\omega\left(\lambda\left(s\,{}_2F_1\left[1, \frac{1}{\omega}; 1 + \frac{1}{\omega}; -\frac{s^\omega}{\mu - 1}\right] - {}_2F_1\left[1, \frac{1}{\omega}; 1 + \frac{1}{\omega}; -\frac{1}{\mu - 1}\right]\right) + \frac{\kappa(\mu - 1)}{\mu} T\right)} = 0 \quad (25)$$

Contrarily, when $\mu < 1$, the root of s situates at the interval between $(1 - \mu)^{1/\omega}$ and 1 (see eq 10), the next equation proves successful

$$\Phi_2^b = \mu s^\omega - (\mu - 1 + s^\omega) \times e^{-\omega\left(\lambda\left(s\cdot{}_2F_1\left[1, \frac{1}{\omega}; 1+\frac{1}{\omega}; -\frac{s^\omega}{\mu-1}\right] - {}_2F_1\left[1, \frac{1}{\omega}; 1+\frac{1}{\omega}; -\frac{1}{\mu-1}\right]\right) + \frac{\kappa(\mu-1)}{\mu}T\right)} = 0 \quad (26)$$

Finally, when $\mu = 1$ and the root of s is again between zero and one ([0,1] interval, see eq 9), we would like to stress that eq 16 multiplied by s^ω seems to be an appropriate form for the numerical root solving procedure

$$\Phi_2' = \frac{1}{\omega}(s^\omega - 1) + \frac{\lambda s}{(\omega - 1)}(s^\omega - 1) + \kappa s^\omega T = 0 \quad (27)$$

Instead of the Newton−Raphson algorithm, the divergence-proof root bracketing method according to Van Wijngaarden-Dekker-Brent (WDB's method in the text)[20] must be applied for the root evaluation of the eqs 25, 26, and 27 (see Figure 2). It is efficient and ensures the convergence as long as the function can be evaluated within range of which it is known to contain the root. The values of nonelementary function ${}_2F_1[a, b; c; z]$ that exist in eqs 25 and 26 and rapidly converge for $z < 0.5$ were calculated with the summation of a number of terms in developed power series to satisfy sufficient accuracy (see Table 2). The accuracy of WDB's method in describing the substrate nondimensionalized concentration according to Φ_2, Φ_2', and Φ_2'' functions was tested, and the relative error was computed as previously described.[10] Data analysis was performed using a modified nonlinear regression computer program[28] implemented in C++. The kinetic parameters were independently calculated also by numerical integration treatment using a nonlinear regression computer program.[29] The CPU times needed for the calculation according to one or the other numerical methods were compared.

4. RESULTS AND DISCUSSION

We have derived implicit equations corresponding to the nondimensionalized variable $s \equiv [S]/[S]_0$ of an enzymatic reaction in the absence or presence of a potent irreversible inhibitor in which substrate utilization and free enzyme inactivation processes can take place according to Schemes 1 and 2. The analysis is based on two assumptions: (i) a steady-state concentration of *ES* is attainable during the entire reaction course and (ii) the value of $1 - 1/\omega$ is a noninteger number. The first assumption is valid when $j[I] \ll k_{+1}[S]$, k_{-1}, k_{+2} and this condition is rarely violated because of very small amount of inhibitor and a great excess of substrate. The second assumption is practically a fact because the ω value is the product of two rates and Michaelis constants whose magnitudes are real numbers, and therefore their composition can be an integer only theoretically. The credibility of integrated rate eqs 16 and 17 (for which $s_\infty = 0$) can be shaken only in the vicinity of a progress curve plateau where the depletion of substrate is obvious. Even this problem can be neglected in the case of very efficient enzymes where its concentration in reaction mixture is smaller than the presicion with which the substrate or product concentration can be measured. However, when this condition is not fulfilled, one has to take into consideration only partial progress curves without plateaus when analyzing them in respect to eqs 16 and 17.

The dependence of implicit functions Φ_1, Φ_1', and Φ_1'' upon s is illustrated in Figure 2. It is obvious at first glance that the Newton−Raphson method based on the derivative calculation is not an appropriate root-solving algorithm which could guarantee the convergence and the correct root evaluation, because the derivatives and values of all three functions in the low boundary proximity of the interval where they are defined become undetermined. Therefore, the rearrangements for all three functions have to be done to avoid these problems, and modified functions Φ_2^a, Φ_2^b, Φ_2', and Φ_2'' are shown in Figure 2. From simple geometry, it is clear that Φ_2'' is almost a straight line. Under these circumstances the Newton−Raphson method rapidly converges toward a close approximation of the solution.[6] But there are two reasons, obvious from Figure 2, why this numerical procedure is not so convincible in the case of functions Φ_2^a, Φ_2^b, and Φ_2'. They are defined at any value of s even at the boundaries of intervals where the true solution exists. However, especially at these points the Newton−Raphson algorithm can fail. The real problem arises at a great time where the true root of s is in the vicinity of the lower boundary and derivatives around those points can increase over all limits. One can also find other critical points inside the root finding interval where the tangent line at a current point shoots off to outer space until it crosses zero. In such a case there is little hope of recovery especially if the particular function is complex outside the interval borders.

For all these reasons, the divergence-proof root bracketing WDB's numerical procedure was applied for the root approximation calculated from eqs 25, 26, and 27 as in our previous work.[15] WDB's algorithm is the method of choice to find a bracketed root of a general one-dimensional function when its derivative cannot be computed easily (see Figure 2), but the function itself is defined within the interval containing the root (see Φ_2^a, Φ_2^b, and Φ_2' in Figure 2). The method combines the sureness of bisection and the speed of a higher-order method[20] which makes it even more justified. All these properties make the applied mixed analytical/numerical approach (WDB's method) relatively fast, and this is the convincing argument about the advantages over direct numerical integration treatment. It has been demonstrated that the computational costs of the direct numerical integration based on a semiimplicit midpoint rule extrapolation method[30] are approximately five times higher than those of the root-finding method according to WDB. The numerical integration method has been developed for solving numerical solutions of stiff systems of differential equations,[29,30] and due to the nature of this integration method, the stepsize in the integration had to be 10 times smaller than in the program using WDB's algorithm (see Appendix in ref 29). For this reason the data analysis applying numerical integration treatment became computationally more intensive and consequently much slower in comparison with WDB's numerical procedure within the same standard deviation.

The Gauss hypergeometric function ${}_2F_1[a, b; c; z]$ of a real variable z occurs in many areas of natural sciences for mathematical description of various processes. The function is a solution of a hypergeometric differential equation and

is expressed as an infinite series (see eq 18). This series is convergent for $|z| \leq 1$ but rapidly converges to the final value only for the case where $|z| \leq 0.5$. For these reasons we have made appropriate linear transformations given in Table 2, being useful for our work. It can be seen from Table 2 that the total number of sufficient terms in a partial sum to attain the required accuracy is controlled by exponential function $w^N/(1 - w)$ except in the last transformation case (for $z > 1.5$) where the function is replaced by $w^N/N(1 - w)$. In this case the convergence is faster, and it has been proven that it compensates the waste of computation time in the range where $z < 2$ or $w = 1/z > 0.5$ (see Table 2).

Simulated progress curves are given in Figure 1. It should be stressed that nondimensionalized variable s at any time was transformed to product concentration variable $[P]_t$, equal to $[S]_0(1 - s)$. The progress curves reveal several interesting properties: (i) initial velocity is always inhibitor concentration independent; (ii) upper progress curves for which $\mu \geq 1$ tends toward the plateau corresponding to the value of $[S]_0$; (iii) progress curves for which $\mu < 1$ reach the plateaus earlier with asymptotes lower than $[S]_0$; the asymptotes decrease with decreasing μ according to eq 10. It should be noted that the following rule plays an important role: μ closer to the unity demands a longer time in which the progress curve reaches the plateau. The first property is not surprising because in all cases where the enzyme−inhibitor complex is not formed instantaneously, as proposed in our kinetic system, the initial rates are inhibitor concentration independent.[13] The properties under (ii) and (iii) are also logical consequences of inhibitor/substrate depletion or of enzyme inactivation, respectively. The plateau is reached earlier in cases where μ is not close to one, and this is the consequence of two different effects. When μ is close to zero and this means that the irreversible inhibitor is in surplus, then the inactivation of enzyme is relatively fast. Contrarily, when μ is high, a part of the enzyme stays intact, and therefore the product formation process can be finished earlier. All these characteristics of simulated progress curves are in full agreement with the original kinetic system in Scheme 2. Moreover, the correctness of the corresponding analytical equations has been crosschecked by numerical integration (see solid lines in Figure 1).

At the end, one could argue about the confidence to the applied entire progress curve analysis in comparison with the classical kinetic analysis. Namely, eq 10 can be linearized by logarithmic algebra and the value $1/\omega$ could be very easily obtained by $log(s_\infty)$ vs $log(1 - \mu)$ plot where $1/\omega$ would be the slope of line diagram. The advantage of such a plot is that the only information needed to construct it are initial and final substrate concentrations (see plateaus in Figure 1). Needed K_M and k_{+2} must be independently evaluated from simple double reciprocal plot, and subsequently, the second-order rate constant j could be calculated from ω. However, there are numerous weaknesses in this procedure,[15] and upon reflection we can see that such an analysis would be reduced only to progress curves where $\mu < 1$. Theoretically the plot of $log(s_\infty)$ vs $log(1 - \mu)$ can be drawn in the μ range from zero to one. But as shown previously, for the case where μ is close to unity the plateau of the progress curve is reached very late, and this is undesirable in practice. On the other hand μ cannot be very small because in such a case the plateau level would be low and could lead to the wrong estimation. Therefore, the classical approach is very inhibitor concentration dependent. Nevertheless, it can be very useful for first diagnostic interpretation of reaction mechanism. Final quantitative progress curve analysis using mixed analytical/numerical method described in this paper, however, appears much more convincing.

ACKNOWLEDGMENT

This work was supported by the Ministry of Education, Science and Sport of the Republic of Slovenia, Grant No. PO-0505-0381.

APPENDIX

(A) Pochhammer's symbol

$$(z)_0 = 1 \tag{28}$$

$$(z)_m = z(z + 1)(z + 2)...(z + m - 1) = \frac{\Gamma(z + m)}{\Gamma(z)} \tag{29}$$

(B) Digamma (Ψ) function is defined as

$$\Psi(z) = \frac{d[ln\Gamma(z)]}{dz} = \frac{\Gamma'(z)}{\Gamma(z)} \tag{30}$$

and

$$\Psi(1) = -\gamma,\ \Psi(m) = -\gamma + \sum_{k=1}^{m-1} k^{-1} \tag{31}$$

γ is Euler's constant and m means an integer number equal to or greater than 2 ($m \geq 2$).

The evaluation of digamma function for a real argument z can be computed by summation of rapidly convergent series[19]

$$\Psi(z) = -\gamma - \frac{1}{z} + \sum_{m=2}^{\infty} (-1)^m \zeta(m) z^{m-1} \tag{32}$$

for $z \leq 0.5$. For z lying in the range between 0.5 and 2 the combination of the following recurrence, reflection and duplication formulas can be applied[19]

$$\Psi(1 + z) = \Psi(z) + \frac{1}{z} \tag{33}$$

$$\Psi(1 - z) = \Psi(z) + \pi ctg(\pi z) \tag{34}$$

$$\Psi(2z) = \frac{1}{2}\Psi(z) + \frac{1}{2}\Psi\left(z + \frac{1}{2}\right) + ln2 \tag{35}$$

Finally for $z \geq 2$ the rapid calculation of $\Psi(z)$ can be done by using an asymptotic formula

$$\Psi(z) = lnz - \frac{1}{2z} - \sum_{m=1}^{\infty} \frac{B_{2m}}{2m} z^{-2m} \tag{36}$$

where B_{2m} are Bernoulli's coefficients.[19]

(C) Primary definition of incomplete beta function is

$$B_z[a, b] = \int_0^z t^{a-1}(1-t)^{b-1}\,dt;\ \mathscr{R}(a) > 0 \qquad (37)$$

but can be represented also as a generalized power series[26]

$$B_z[a, b] = \tilde{B}_1 + \tilde{B}_2 \qquad (38)$$

where

$$\tilde{B}_1 = \frac{\Gamma(a)\Gamma(1-a-b)z^a(-z)^{-a}}{\Gamma(1-b)} \qquad (39)$$

$$\tilde{B}_2 = \frac{z^a(-z)^{b-1}}{a+b-1}\sum_{m=0}^{\infty}\frac{(1-b)_m(1-a-b)_m}{(2-a-b)_m m!}z^{-m} \qquad (40)$$

for $|z| > 1 \wedge a + b \notin \mathbb{N}^+$.

REFERENCES AND NOTES

(1) Michaelis, L.; Menten, M. L. Die kinetik der invertinwirkung. *Biochem. Z.* **1913**, *49*, 333−369.
(2) Fersht A. In *Structure and Mechanism in Protein Science*; Freeman: New York, 1999.
(3) Segel I. H. In *Enzyme Kinetics*; Wiley-Interscience: New York, 1993.
(4) Lineweaver, H.; Burk, D. The determination of enzyme dissociation constants. *J. Am. Chem. Soc.* **1934**, *56*, 558−566.
(5) Orsi, B. A.; Tipton, K. F. Kinetic Analysis of Progress Curves. *Methods Enzymol.* **1979**, *63*, 159−183.
(6) Duggleby, R. G. Analysis of Enzyme Progress Curves by Nonlinear Regression. *Methods Enzymol.* **1995**, *249*, 61−90.
(7) Duggleby, R. G.; Morrison, J. F. Progress curve analysis in enzyme kinetics model discrimination and parameter estimation. *Biochim. Biophys. Acta* **1978**, *526*, 398−409.
(8) Marcus, M.; Plesser, T. In *Kinetic Data Analysis*; Endrenyi, L., Ed.; Plenum Publishing: New York, 1981; pp 317−339.
(9) Laidler, K.; Bunting, J. In *The Chemical Kinetics of Enzyme Action*; Calderon Press: Oxford, 1973; pp 163−180.
(10) Goudar, C. T.; Sonnad, J. R.; Duggleby, R. G. Parameter Estimation Using a Direct Solution of the Integrated Michaelis−Menten Equation. *Biochim. Biophys. Acta* **1999**, *1429*, 377−383.
(11) Stojan, J.; Pavlič, M. R. On the inhibition of cholinesterase by D-tubocurarine. *Biochim. Biophys. Acta* **1991**, *1079*, 96−102.
(12) Goličnik, M.; Stojan, J. Transient kinetic approach to the study of acetylcholinesterase reversible inhibition by eseroline. *J. Enzym. Inhib. Med. Chem.* **2002**, *17*, 279−285.
(13) Morrison, J. F.; Walsh, C. T. The behaviour and significance of slow binding enzyme inhibitors. *Adv. Enzymol.* **1988**, *61*, 201−301.
(14) Goličnik, M.; Stojan, J. Multistep analysis as a tool for kinetic parameter estimation and mechanism discrimination in the reaction between tight-binding fasciculin2 and electric eel acetylcholinesterase. *Biochim. Biophys. Acta* **2002**, *1597*, 164−172.
(15) Goličnik, M. On a nonelementary progress curve equation and its application in enzyme kinetics. *J. Chem. Inf. Comput. Sci.* **2002**, *42*, 157−161.
(16) Briggs, G. E.; Haldane J. B. S. A note on the kinetics of enzyme action. *Biochem. J.* **1925**, *19*, 338−339.
(17) Duggleby, R. G. Quantitative analysis of the time courses of enzyme-catalysed reactions. *Methods* **2001**, *24*, 168−174.
(18) Erdelyi, A.; Magnus, W.; Oberhettinger, F.; Tricomi, F. G. In *Higher Transcendental Functions*; McGraw-Hill: New York, 1953; p 1.
(19) Abramowitz, M.; Stegun, I. A. In *Handbook of Mathematical Functions*; National Bureau of Standards, Dover Public: New York, 1970; pp 556−565.
(20) Press: W. H.; Teukolsky, S. A.; Vetterling, W. T.; Flannery, B. P. In *Numerical Recipes in C*; Cambridge University Press: Cambridge, 1992; pp 208−211, 271−273.
(21) Jeandel, E. Évalution rapide de fonctions hypergéométriques. *Rapport technique INRIA* **2000**, no. 0242.
(22) Karatsuba, E. A. Fast evaluation of transcendental functions. *Problemy Peredachi Informatsii* **1991**, *24*, 76−99.
(23) Karatsuba, E. A. Fast evaluation of hypergeometric function by FEE. In *Computational Methods and Function Theory*; Papamichael, N., Ruscheweyh, S., Saff, E. B., Eds.; World Scientific Publishing: London, 1999; pp 303−314.
(24) Karatsuba, E. A. Fast computation of some special integrals of mathematical physics. In *Scientific Computing, Validated Numerics, Interval Methods*; Krämer, Von Gudenberg, W., Eds.; Kluwer Academic/Plenum Publishers: New York, 2001; pp 29−40.
(25) Forrey, R. C. Computing the hypergeometric function. *J. Comput. Phys.* **1997**, *137*, 79−100.
(26) http://www.functions.wolfram.com.
(27) Wolfram, S. In *Mathematica*; Addison-Wesley Publishing Company: New York, 1993; p 106.
(28) Duggleby, R. G. Regression Analysis of Nonlinear Arrhenius Plots: an Empirical Model and a Computer Program. *Comput. Biol. Med.* **1984**, *14*, 447−455.
(29) Stojan, J. Analysis of Progress Curves in an Acetylcholinesterase Reaction: A Numerical Integration Treatment. *J. Chem. Inf. Comput. Sci.* **1997**, *37*, 1025−1027.
(30) Bader, G.; Deuflhard, P. A. A Semiimplicit Mid-Point Rule for Stiff Systems of Ordinary Differential Equations. *Num. Math.* **1983**, *41*, 373−398.

CI0304021